Communication in Physical Sciences, 2024, 11(2): 188-206

Graphical Abstract

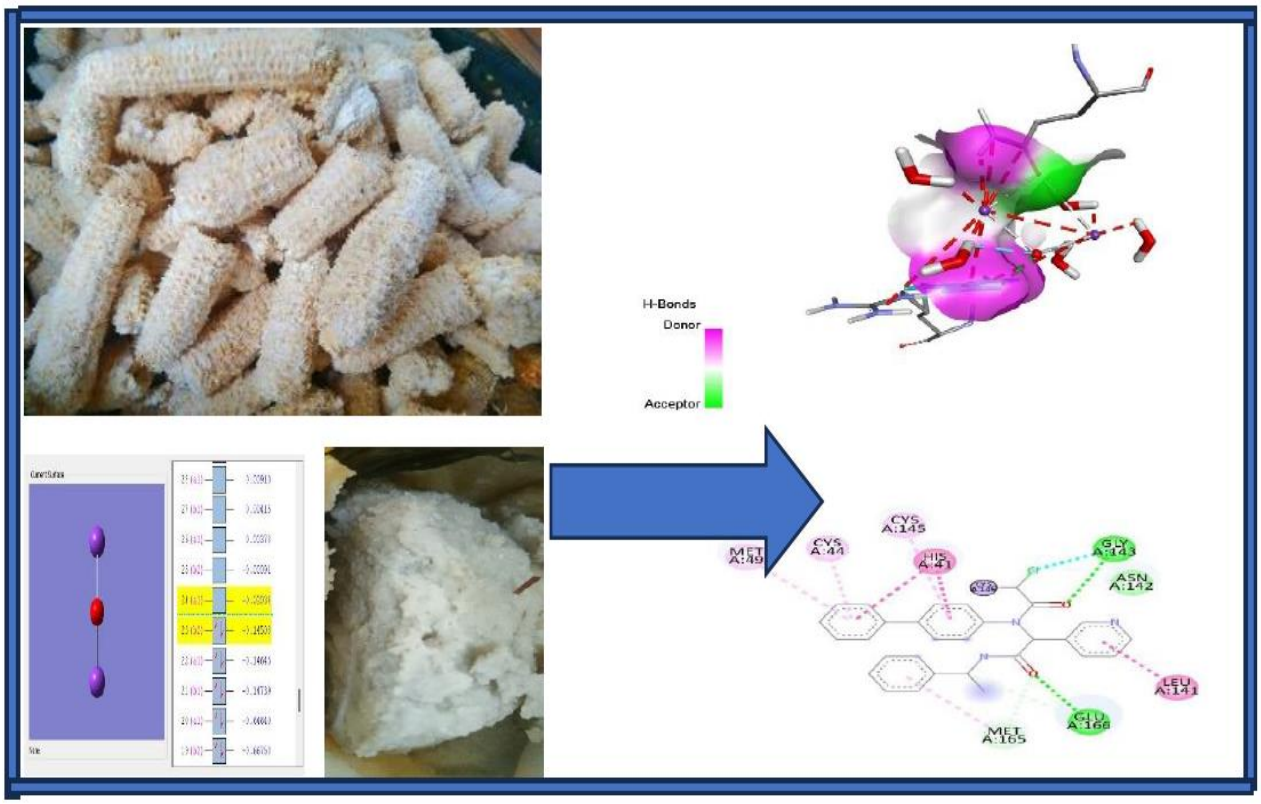

Communication in Physical Sciences, 2024, 11(2): 188-206

Valorization of an Agricultural Waste-Corncob: Investigation of Potassium Oxide from Corncob Ash Crystals as an Antiseptic and Disinfectant Agent

Henrietta Ijeoma Kelle and Musa Runde*
Received: 18 October 2023/Accepted: 18 April 2024 /Published: 24 April 2024

Abstract: *Antiseptics play a crucial role in upholding hygiene standards and curbing the transmission of diseases. Corn cob ash has been utilized to uphold cleanliness and ensure hygiene, particularly in low-income communities. The combustion of corn cob biomass yielded corn cob ash crystals, whose composition was analyzed using X-ray Fluorescence Spectroscopy. Predominantly, potassium oxide constitutes 80.69% of these crystals. This research investigates the antibacterial and disinfectant properties of potassium oxide crystals derived from corn cob ash. Their effectiveness against various microorganisms was compared with benzalkonium chloride and ampicillin, the industry standards. Using density functional theory and molecular docking, the reactivity and interaction of the compound with specific bacteria and SARS-CoV-2 proteins were explored. Geometric analysis employing DFT revealed significant alterations in bond lengths and angles of the potassium oxide molecule due to solvent presence. Notably, a promising interaction between the substance and the SARS-CoV-2 protein suggests its potential application in developing antiseptics and hand sanitizers.*

Keywords*: Corncob ash crystals, Benzalkonium chloride, Hand sanitizer, Ligand, Molecular docking, and Protein binding site.*

Henrietta Ijeoma Kelle
Department of Chemistry, National Open University of Nigeria, Jabi, FCT, Abuja, Nigeria
Email: hkelle@noun.edu.ng
Orcid id: 0000-0003-3701-4652

Musa Runde
Department of Chemistry, National Open University of Nigeria, Jabi, FCT, Abuja, Nigeria
E-mail: rmusa@noun.edu.ng
Orcid. Id: 0000-0001-9312-0455

1.0 Introduction

Antiseptics play a vital role in general hygiene and the prevention and management of diseases. They are chemical agents used to inhibit or kill microorganisms on living tissues, surfaces, or objects (McDonnell G. and Rusell, 1999). Antiseptics work by disrupting the structure or function of microorganisms such as bacteria, viruses, fungi, and protozoa. They can prevent the growth and spread of these pathogens, reducing the risk of infection. These properties can be utilized in the preparation of personal hygiene agents such as hand sand sanitisers (McDonnell and Rusell, 1999). Alcohol and chlorhexidine are effective in killing a wide range of microorganisms and are particularly important in situations where soap and water are not readily available (Hernandes, *et al*, 2004). Furthermore, antiseptics are frequently used in wound care to prevent infection. They can be applied to the skin around the wound or used directly on the wound, depending on the severity and type of wound (Akita, *et al*, 2022). Antiseptic solutions or ointments can help clean the wound and inhibit the growth of bacteria. The disinfection ability of antiseptics is important in medical procedures, especially during surgery. Antiseptics are valuable in settings where the risk of disease transmission is high, such as hospitals, nursing homes and public places

(Ahmad, *et al*, 2018). While antiseptics are effective in controlling and preventing infections, it is important to note that they have limitations. Some microorganisms may be resistant to certain antiseptic agents, and improper or excessive use of antiseptics can lead to skin irritation or other adverse effects (Ghafoor, *et al*, 2022, Chen, *et al*, 2021) and sometimes the alcohol content may be forbidden in some religious right. It is essential to search for more new compounds with antiseptic properties to mitigate the challenges of antiseptic resistance, skin irritation and incompatibility with the target surface or skin. This work is targeted at identifying the antiseptic or disinfectant properties of corn cob ash crystals which will serve as a supplement to the existing antiseptics in the market. This will be achieved through analyzing the antimicrobial activities of the previously prepared corn cob ash crystals on selected bacteria while comparing these effects with the activities of Benzalkonium chloride as standard. Furthermore, the interaction mechanisms between the test sample and the standard will be studied on selected bacteria and SARS-CoV-2 proteins using Pryx and Biovia software.

Corncob, a waste product of agricultural activities is usually generated in huge quantities, and discarded on farmlands, especially in developing countries. They can eventually enter surface water through surface runoff, whereby they constitute a menace and can cause water pollution. Corncob is known for its potential as a source of renewable energy and is often used in gasification and combustion processes (Laohalidonand, *et al*, 2017). However, recent studies have also shown that corn cob ash has antiseptic properties that can be used in various applications, on the other hand, ash from other organic materials such as fly ash has flexural behaviour (Elegbede, *et al*, 2021, Kistan, *et al*, 2023). The highly alkaline nature of corn cob ash is particularly effective in inhibiting the growth of microorganisms (Melo-Silveira, *et al*, 2011). According to (Eno, *et al*, 2023), phytochemicals and prebiotic potential found in sweet corn cob provide significant health benefits to human consumption, and act as an antioxidant, antimicrobial, anticoagulant, anticancer, and aids in reducing blood glucose levels (Eno, *et al*, 2023). Thus, this suggests the potential of corncob ash as a safer and more sustainable alternative to synthetic antiseptics in wound care products and disinfectants.

In furtherance to this research, high alkaline crystals were obtained from corn cob ash previously prepared by burning the corn cob biomass in an open ventilated space to ensure total combustion and later process to crystals. The composition of the crystals was determined using X-ray Fluorescence Spectroscopy and the analysis of the Density Functional Theory (DFT) was carried out computationally as described by (Eddy and Ita, 2011; Obi, 1990). The reactivity, stability, excitations, and intermolecular interaction of the compound under study are revealed by the results obtained from Frontier Molecular Orbital (FMO); analysis of the energy of the Highest occupied molecular orbital (HOMO) and the Lowest unoccupied molecular orbital (LUMO). The bond nature, charge transfer, stability, and reactivity of the compound were determined using Natural bond orbital elucidation.

2.0 Materials and Methods

2.1 Materials

The materials used in the experimental studies include Corn cob biomass, distilled water, pH meter, and other laboratory glass wares.

Muller Hinton Agar (MHA), Muller Hinton Broth (MHB), MacFarland standard, distilled Water, measuring cylinder, conical flasks, Petri dishes, spatula, cork borer, autoclave, water bath, laminar flow hood, weighing balance, incubator, standards (ampicillin and benzalkonium chloride) and test organisms. Other requirements for computational analysis are the common computational software such

as ChemDraw, GausView 6.0 and Gaussian 09W, and molecular docking software (Biovia 1sp and Pyrex). The proteins used in this work are 5iip, 5wze, 1dih and 7 rn1.

2.2 Methods

2.2.1 Preparation of Corn cob crystal

Corn cob biomass (agricultural waste) was obtained in the open field farm at Girei Local Government of Adamawa State. 5 kg of the biomass was burnt in an open basin until ash was formed. 500 g of the ash was dissolved in 500 ml of distilled water in a 1000 ml capacity beaker and allowed to stand at room temperature for 24 hours. The solution was then filtered using a 0.5d mesh sieve and this process was repeated at each state testing the alkalinity of the residue with a pH meter when the meter reading was 7.8 the process was said to be completed. Note that the alkalinity test was used to monitor the endpoint of the filtration process, the researcher was not interested in monitoring the change in pH of the residue with time.

The filtrate is further filtered using Whatman filter paper and kept at room temperature until required. The filtrate is boiled at 100 ^{0}C until a reasonable volume of the filtrate is reduced this also is necessary to increase the concentration of the solute. The boiled solution is then allowed to cool under room temperature which later is transferred to a 100 ml beaker, covered with a mesh to prevent contamination with particles but allowed the solvent to evaporate (air-dried) for 48 hours. the solid crystals were seen to appear first at the bottom of the beaker within 48 hours and were transferred into a refrigerator for 24 hours. White crystals were observed developing from the bottom and spreading around the walls of the beaker. These crystals were later separated from the water by decantation and eventually dried an ovum at 100 ^{0}C until constant weight was observed. Note also that, the drying was not intended to study the water of crystallization of the sample.

2.2.2 Compositional analysis

The composition of the crystals was determined using X-ray Fluorescence Spectroscopy. The equipment (X-Supreme 8000) was calibrated using reference standards and equipment working conditions prior set at a time of 300 s at 5 kV, 183 765 lA; and a measuring time of 60 s at 12 kV, 584 lA. Thereafter sample was transload on the autosampler tray in the XRF, and different groups of elements were analyzed with varying condition detectors. Data acquisition in this study was acquired by the software attached installed on the data station (Kareem, *et al*, 2010).

2.2.3 Antimicrobial Susceptibility Test

The sample was evaluated against the test microorganisms using the agar-well diffusion method as described by (Schulte *et al*, 2014) with slight modification. Clinical isolates of *Staphylococcus aureus*, *Pseudomonas aeruginosa* and *Escherichia coli* were sub-cultured in Muller Hinton Broth (MHB), these were incubated for 24 hours at 37ºC the turbidity of the cultures was adjusted to MacFarland standard using sterile Muller Hinton Broth. The organisms were seeded separately on solidified Muller Hinton Agar (MHA) plates. Wells were bored on each of the culture media using a sterile (6mm) cork borer. The sample was constituted with Dimethyl Sulphoxide (DMSO) and tested at concentration levels of 500mg/ml, and 250 mg/ml. 125 and 62.5 mg/ml. Fixed volumes (100µl) of the constituted sample were separately introduced into equidistant wells (6mm) bored on the surface of the Muller Hinton Agar plates, which had been previously seeded with the test organisms. DMSO was used as the negative control while Ampiclox and Benzalkonium chloride were used as positive control. incubation, the seeded plates containing the test sample were first kept in the refrigerator for about 15 minutes to enhance the diffusion of the agent while the organisms were

temporarily inactivated, after this the plates were incubated at 37 ^{o}C for 24 h.
After 24 hours of incubation, the plates were observed for clear zones of inhibition around the well containing the extracts. The presence of a clear zone of Inhibition surrounding the wells was measured with a ruler and recorded in millimetres (mm) as shown in Table 2.

2.3 Computational approach
2.3.1 Density Functional Theory (DFT)

GaussView 6.0 and Gaussian 09W were used, to put up the compound's geometry and calculate its electron structure respectively. These display the compound's electron structure as well as the location of the two potassium atoms and their connections to the oxygen atom. The DFT calculation's basis selection is 6-311G $^{++}$(2p,2d). The electron-electron interaction in the system was represented using the Local Density Approximation (LDA). The initial geometry is subjected to an energy reduction procedure to identify the compound's most stable configuration using the optimization technique, and this process is repeated until the equilibrium position that reduces the system's overall energy is discovered. Calculations were made for the compound's electrical density and other parameters including bond length and angle. The same theoretical methodology was used to calculate Natural Bond Orbitals (NBO) using the NBO software 3.1 integrated into Gaussian.

2.3.2 Docking approach

Pyrex was used in this study to analyze how proteins and ligands interact, and the Biovia Discovery Studio software made it easier to see how protein receptors and interactions work. The Research Collaboratory for Structural Bioinformatics (RCSB) from Protein Data Bank and Yorodumi browser for structure data provided the targeted protein structures, 5iip (*Staphylococcus aureus*), 5wze (*Pseudomonas aeruginosa*), 1dih (*Escherichia coli*) and 7rn1(SARS-CoV-2 (COVID-19), in Protein Data Bank (PDB) format (Peng, *et al*, 2017, Ma, *et al*, 2021, Olafusi, *et al*, 2018) as shown in Figs 4,7,10 and 12.
Using Pyrx, the proteins, ligands, and their interactions were prepared in situ. The Biovia Discovery Studio was also used to show the different linkages and interatomic interactions. For comparison tests, the standard ingredient of a non-alcohol-based hand sanitizer was Benzalkonium chloride. This common substance was likewise exposed to docking with the proteins as indicated above.

3.0 Results and Discussion
3.1 Results

The experimental and computational results of the compositional, antimicrobial, computational and molecular interaction of potassium oxide with these organisms are presented in Table 1 and Fig. 1 below.

Table 1: Composition of corn cob ash crystals

Compound	C (%)
K_2O	80.69
SiO_2	9.31
P_2O_5	5.83
Cl^-	2.02
SO_3^{-2}	1.75
Al_2O_3	0.20
Rb_2O	0.15
Fe_2O_3	0.05

Fig. 1: Corncob ash crystals

Corn cob ash predominantly consists of inorganic elements formed during the combustion process. Its mineral content encompasses various essential components, notably potassium (K), calcium (Ca), magnesium (Mg), phosphorus (P), and silicon (Si), along with trace amounts of iron (Fe) and zinc (Zn) (Yao, *et al*, 2018). The precise constitution of corn cob ash can differ, contingent on factors like the specific type of corn cob and the conditions under which combustion occurs (Wojcieszak, *et al*, 2022). From the X-ray fluorescence result of the analysis of the crystal obtained from the corn cob ash (Fig. 1), the predominant compound is potassium oxide (K_2O), accounting for 80.69% of the composition, followed by silicon oxide (SiO_2) at 9.31%. Other compounds present include P_2O_5 (5.83%), chlorine (Cl) (2.02%), sulfur trioxide (SO_3) (1.75%), aluminum oxide (Al_2O_3) (0.20%), rubidium oxide (Rb_2O) (0.15%), and iron oxide (Fe_2O_3) (0.05). It is evident from these findings that the antimicrobial properties of these crystals can be attributed to the leading compound K_2O.

Table 2: Antimicrobial analysis of potassium oxide

C (mg/ml)	**Organism**	***Staph. aureus***	***Escherichia coli***	***P. aeruginosa***	**+Ve Control (Ampiclox)**	**Benzalkonium chloride**	**-ve Control DMSO**
500	*i(mm)*	13.00	11.00	Too large	Too large	16.0	NI
500	*ii(mm)*	14.00	11.00	Too large	Too large	15.0	NI
500	*iii (mm)*	13.50	11.00	Too large	Too large	14.0	NI
250	*i(mm)*	11.00	NSI	42.0	42.0	14.0	NI
250	*ii (mm)*	11.00	NSI	42.0	42.0	14.0	NI
250	*iii (mm)*	11.00	NSI	42.0	42.0	14.0	NI
125	*i(mm)*	NSI	NI	31.0	31.0	14.0	NI
125	*ii (mm)*	NSI	NI	31.0	31.0	NSI	NI
125	*iii (mm)*	NSI	NI	31.0	31.0	NSI	NI
62.5	*i (mm)*	NI	NI	17.0	17.0	NSI	NI
62.5	*ii (mm*	NI	NI	16.0	16.0	NSI	NI
62.5	*iii (mm)*	NI	NI	16.5	16.5	NSI	NI

****Diameter of cork borer (6mm) included in the above result, i. first reading, ii second reading, iii. average plate reading, NSI - No significance inhibition, NI -No inhibition and DMSO- Dimethylsulfoxide**

The disparities in the composition of the crystals under study and the ones reported by (Yao, *et al*, 2018), could be attributed to the process involved where in this work crystallization was the priority while the latter was strictly ashing of the corncob biomass. Another possible reason could be related to the species of the corncob and the environment where the crop was produced.

The result of the activities of the Potassium Oxide (K_2O) and Benzalkonium chloride (second standard) at different concentrations against *Staph. Aureus Escherichia coli* and *P. aeruginosa* is presented in table 2. Potassium Oxide and Benzalkonium chloride (second standard) were active on all the microorganisms at a high concentration of 500 mg/ml.

At this concentration the standard drug Ampicillin was high as such, no clear zone was observed on the plate. The test compound and the second standard continued to exhibit activity significantly at 250 mg/ml on Staphylococcus aureus while no significant activities were recorded at the same concentration against *Escherichia coli* and *P. aeruginosa.* While the nonsignificant activity of these two compounds persisted on the *staph. Aureus* at 62.5 mg/ml activities were not observed on the *Escherichia coli* and *P. aeruginosa* at the same concentration as the test compound. The result shows that the standard drug ampicillin is more active than the test compounds and the second standard on all the microorganisms subjected to this analysis.

3.2 Geometrical study

Table 3 shows the geometrical study of K_2O in three different solvents (ethanol, aqueous and Dimethyl Sulphuroxide) where the gaseous phase is use as a reference to determine the changes in the geometry of the compound concerning different mediums.

Geometric investigations of a chemical can reveal significant information about its composition, properties, and behaviour. The spatial configuration of the atoms in potassium oxide is explored and analyzed in geometric research. Understanding the three-dimensional structure of the substance and how it interacts with other molecules or proteins depends on this. The investigated structure underwent conformational analysis, and the DFT approach was used to optimize the most stable conformation. K_2O gas phase bond length and angle served as the benchmark for comparison with the other solvents, including DMSO, H_2O, and ethanol.

Table 3: Structural geometry of potassium oxide in different solvents; (K_2O Etol, K_2O DMSO, K_2O H_2O and K_2O in gas phase)

Bond label	K_1- O_2	K_1-O_2-K_3 (Angle in ^{0}C)
K_2O-gas (Å)	2.222075	179.99420
K_2O-ethanol (Å)	2.44342	154.80048
K_2O-Water (Å)	2.46002	113.55440
K_2O-DMSO (Å)	2.45683	114.5713

To test the impact of solvents on the angle and length of the bonds between the atoms in K_2O, the bond length and angle were measured in the gas phase and three solvents: DMSO, Ethanol, and Water. The results show that both the bond length and the bond angle of the K_2O are significantly influenced by the various solvents used in this investigation. For results on bond length and angle, see Table 3. The bond length of K-O is 2.222075 in the standard (gaseous phase), 2.45683 in DMSO, 2.44342 in Etol and 2.46002 in Water. The bond angles for DMSO, Etol, Water, and Standard are 114.5713, 154.80048, 113.55440, and 179.99420, respectively. This study showed that the solvent has considerable influence on the K_2O and that these changes may change the compound's chemical behaviour. The result also shows that the reference structure which is represented in the gas phase is planner while the effect of the

aqueous solvent was much on the bond angle. An increase in bond length will result in to decrease in stability and the compound will be more reactive. From this result, K_2O+H_2O will be more reactive owing to its increase in the bond length compared to K_2O in Etol and DMSO. On the other hand, a large bond angle results in less steric hindrance thereby allowing other molecules to interact with the solute. This also means that K_2O+ Etol and K_2O in the gas phase have less steric hindrance and will show more interactivity with other molecules. In total perspective, longer bond lengths typically indicate weaker interaction while shorter bond lengths indicate stronger bonds. Weaker bonds are easier to break while stronger ones need more energy to break

3.2 Frontier Molecular Orbital (FMO)

The energy gap diagrams of the molecular orbital of Potassium Oxide in various solvents which includes; Water (K_2O + H_2O), Ethanol (K_2O + Ethanol), Dimethylsulphuoxide and (K_2O + DMSO) are presented in Figs. 2 to 4 below.

The HOMO-LUMO orbitals of potassium oxide (K_2O) are the main subject of investigation since they are essential for comprehending the electronic structure and reactivity of the molecule. These orbitals' energies, characteristics, and other pertinent aspects of the electrical structure are all covered in great detail (Table 4). The energy of the most energetically accessible electrons in the molecule is represented by the HOMO (Highest occupied molecular orbital) energy level, which is found to be 0.10455. In contrast, the energy level of the LUMO (Lowest unoccupied molecular orbital), which represents the energy of electrons accessible to accept incoming electrons during chemical processes, is calculated to be 0.02968 eV.

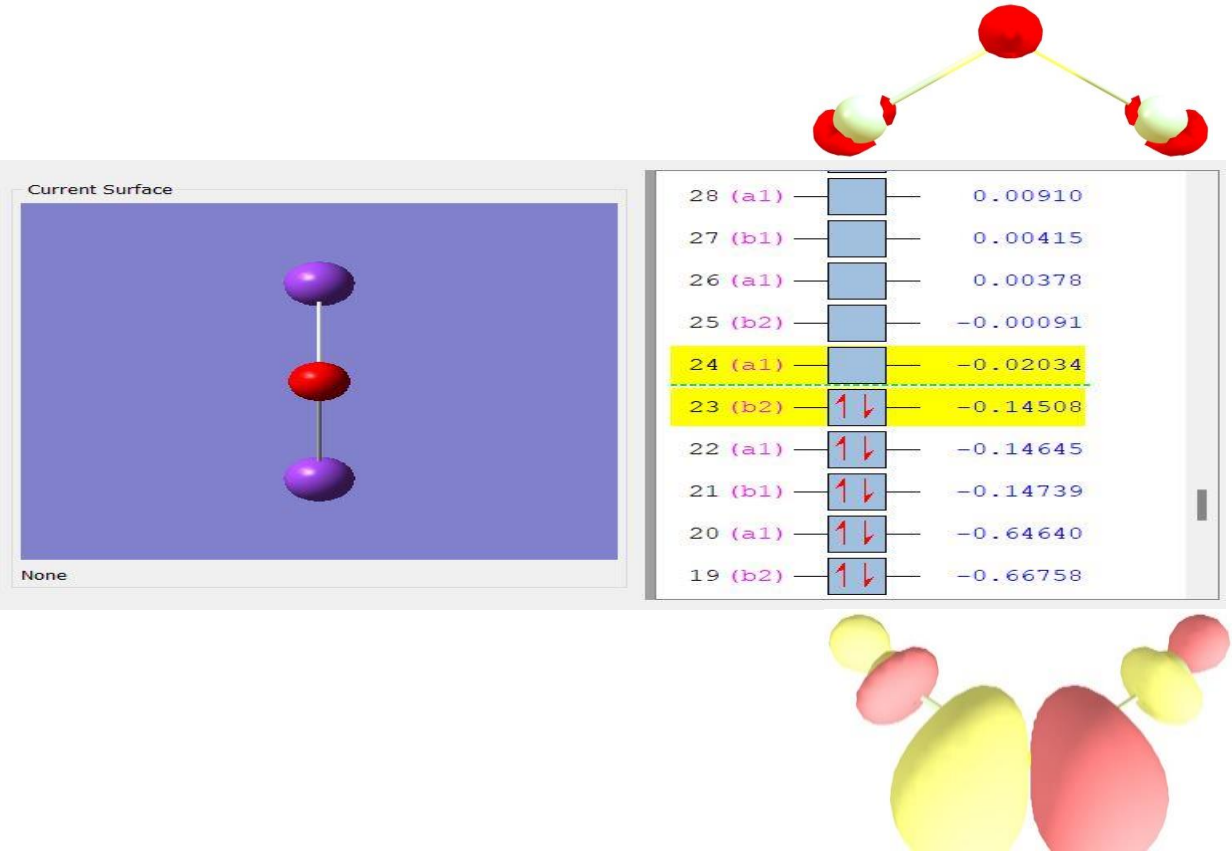

Fig.2: K_2O + DMSO (HOMO/LUMO Energy gradient)

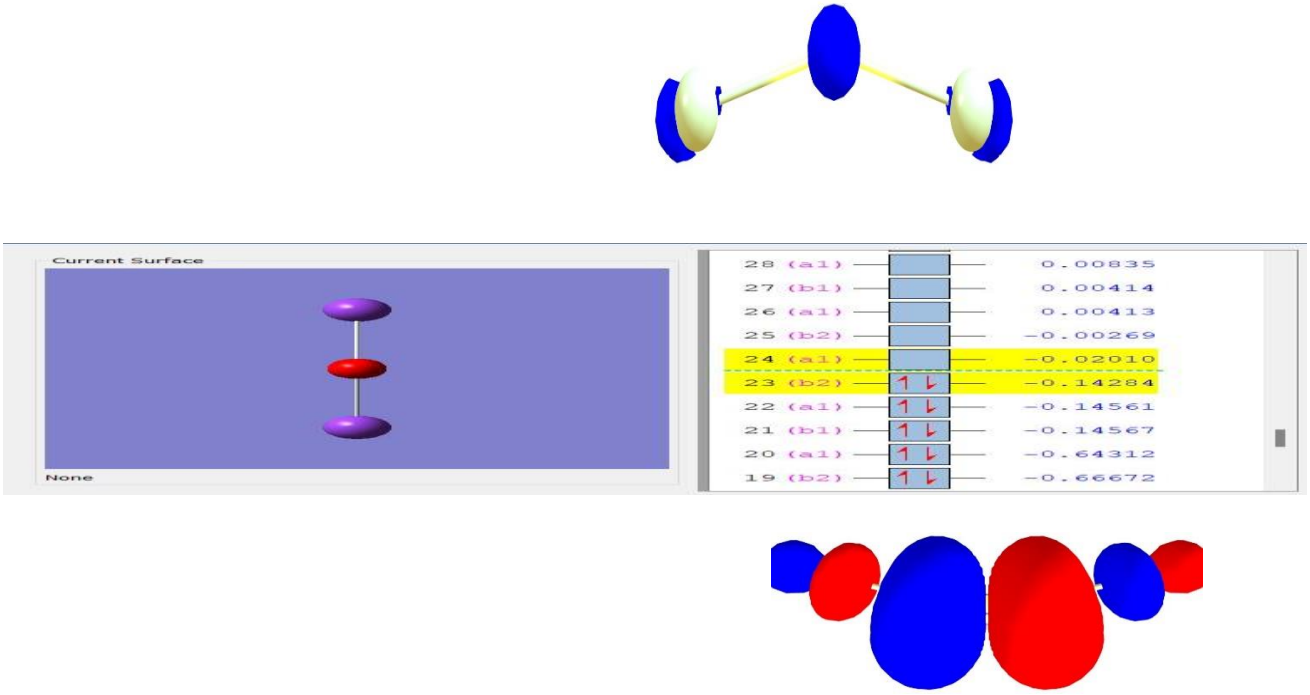

Fig. 3: K_2O+Ethanol (HOMO/LUMO Energy gradient)

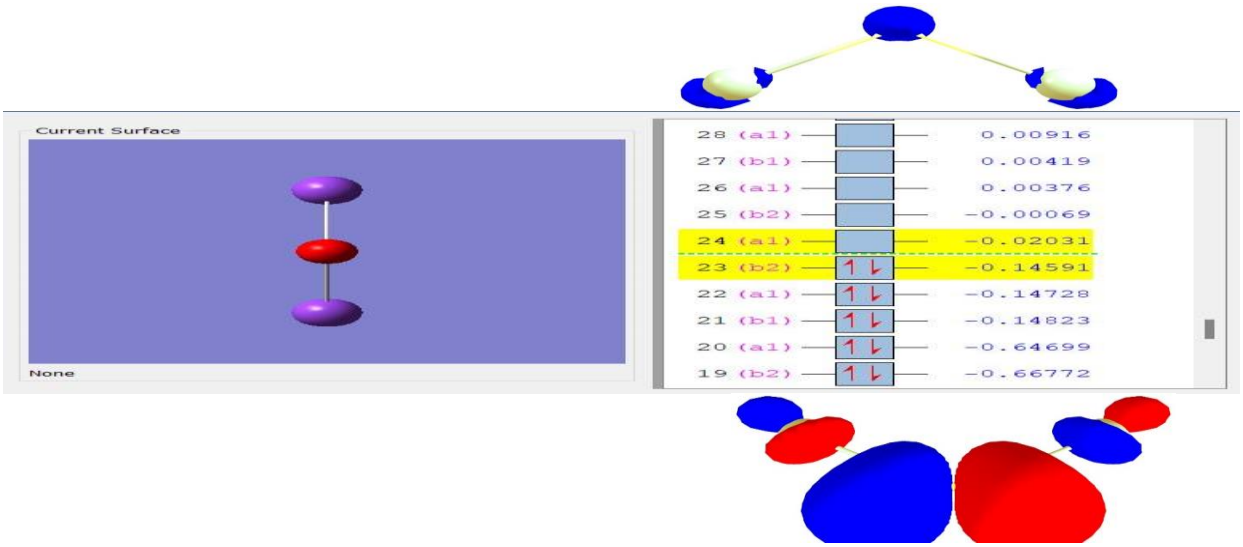

Fig.4: K_2O+H_2O (HOMO/LUMO Energy gradient)

The energy needed to remove an electron from the HOMO and the likelihood that the molecule will lose an electron and transform into a cation is both indicated by the ionization potential (IP), which is predicted to be 2.84495 eV. The energy needed to add an electron to the LUMO and the propensity of the molecule to gain an electron and form an anion is represented by the electron affinity (EA), which is discovered to be -0.80763 eV (negative value of LUMO energy level).

Table 4: Some quantum descriptors

Quantum descriptors	Value
E_{HOMO} (eV)	-0.1046
E_{LUMO} (eV)	-0.0230
Energy gap (eV)	2.0373
Ionization potential (, IP in eV)	2.8450
Electron affinity (EA in eV)	0.8076
Molecular softness (σ in eV)	0.4908
Molecular hardness (η in eV^{-1})	1.0187
Chemical potential (μ in eV)	-1.8263
Electrophilicity (ω)	1.6371
EFL	1.8262

The energy needed for electronic transitions within the molecule is indicated by the energy gap of 2.037318 (about 2.04) between the HOMO and LUMO levels. A wider energy gap denotes increased stability and decreased reactivity (Eddy *et al*., 2023). The mathematical inverse of the ionization potential, or Chemical Softness value, is calculated to be 0.4908842. A lower value denotes increased reactivity and chemical softness. The chemical hardness, which measures a molecule's resistance to either giving or receiving electrons, is given as 1.018659 (= IP - EA). The Chemical Potential of -1.82629, which gauges the molecule's capacity to donate electrons, is also provided by the HOMO-LUMO analysis.

Table 5: Analysis Of The Natural Bond Orbital Interactions

Compound	Donor	Acceptor	E^2 (Kcal/mol)	EGJ– E(J)	F(i.j)
K_2O gas.	б O	LP K_1	4.12	0.31	0.032
	LP O_1	LP* K_1	2.53	1.01	0.045
	LP O_1	LP* K_3	1.65	0.23	0.017
K_2O H_2O	LP O_1	LP* K_2	1.80	1.12	0.40
	LP O_1	LP* K_2	1.14	0.36	0.018
	LP O_1	LP* K_3	1.18	0.26	0.016
K_2O DMSO	LP O_3	LP* K_1	1.19	0.26	0.16
	LP O_3	LP* K_1	1.42	0.33	0.019
	LP O_3	LP* K_1	1.81	1.11	0.40
K_2O CH_3CH_2 OH	LP O_3	LP* K_1	1.82	1.10	0.040
	LP O_3	LP* K_1	1.22	0.26	0.016
	LP O_3	LP* K_1	1.27	0.35	0.019

Also, the electrophilicity index for potassium oxide is 1.637127, indicating its propensity to receive electrons during chemical reactions. The compound's 1.826293 electron flow length (EFL), which is related to how electrons are transferred inside molecules, is measured. These findings, which cover energy levels, ionization potential, and electron affinity, provide crucial insights into the electrical structure, reactivity, and stability of potassium oxide.

The chemical softness and hardness provide information on the substance's capacity for electron donation and acceptance, while the electron affinity values shed light on its reactivity. The behaviour of the molecule in chemical reactions and electron transfer procedures can also be described using the electrophilicity index and electron flow length. From the data presented in the table, the most significant stabilization energy within the molecule for each of the listed compounds is 4.12 kcal/mol, arising from the interaction between б O →LP K1. The next highest stabilization energies are 2.53 kcal/mol and 1.65 kcal/mol, resulting from LP O1 →LP* K1 and LP O1 →LP* K3 interactions, respectively, for the K_2O gas phase. For K_2O in the presence of H_2O, the highest donor-acceptor interactions are observed as LP O1 →LP* K2 (1.8018 kcal/mol), LP O1 →LP* K2 (1.1418 kcal/mol), and LP O1 →LP* K3 (1.18 kcal/mol). In the case of K_2O with Etol, similar donor and acceptor groups result in LP O3 →LP* K1 interactions, with respective stabilization energies of 1.82 kcal/mol, 1.22 kcal/mol, and 1.27 kcal/mol. Similarly, for K_2O with DMSO, the donor and acceptor group show varying high stabilization energy, with LP O3 →LP* K1 having energies of 1.19 kcal/mol, 1.42 kcal/mol, and 1.81 kcal/mol. These results indicate that Potassium Oxide in the gas phase exhibits the strongest stabilization energy, making it highly interactive with surface microorganisms. The high stabilization energy in the gas phase suggests a stable molecular structure and efficient charge transfer within Potassium Oxide's molecules.

3.3 Molecular docking

In this study, molecular docking was explored to study the interactions between various ligands and receptors of the proteins isolated from the microorganisms subjected to this test. The interaction revealed the possibilities of using Potassium Oxide as antiseptics and by extension use for the formulation of household and occupational antiseptics like hand sanitizers. To achieve our goal, proteins of 7rni; SARS-CoV-2 (COVID-19), 5iip; *Staphylococcus aureus*, 5wze; *Pseudomonas aeruginosa* and 1dih; *Escherichia coli* were docked against the compounds under study; Potassium Oxide, and the standard being used in the formulation of non-alcohol-based hand ssanitiser and antiseptics, Benzalkonium chloride. Ligand-protein interaction with a considerable number of hydrogen bonds is considered to exhibit microbial activity against the test organism bearing the protein. From the geometrical study of the sample, the addition of solvent is shown to have a significant effect on the chemical properties of the sample. Therefore, it was critical to study the ligan-protein interactions of the sample in different samples which include: DMSO, Water and Ethanol. The availability of binding sites on the proteins was also elucidated using Biovia software. This data is used to identify the possible sites that could interact with the ligands and it is conducted as part of the pre-docking procedure when using Pyrx for the molecular docking.

3.4 Pre-docking results; Protein Binding sites

The binding sites on the protein subjected to this work were identified and the results show that 5iip (*Staphylococcus aureus*) has four chains (A, B, C and D). The pre-docking analysis was necessary for selecting the chain with the highest number of binding sites which will yield to more interactivity. All the chains show potential to form conventional hydrogen bonds with ligands. However, chain A contains one conventional hydrogen bond (Val 284) and one alkyl bond (263), whereas, Chains B, C and D contain two hydrogen bonds each; (PHE 283, VAL 288), (VAL 345, PRO 343) and (VAL 345, PRO 343) respectively. Other bonds are alkyl bond for chain B; ALA 270, LEU 310, ALA 265 ILEU 282 and VAL 284, for chain C; VAL 345 while for chain D; one alky bond VAL 342 and a Carbon-Hydrogen bond Val 344. Consequently, Chain “D” was selected for

the molecular docking studies with the sample ligands due to the additional availability of a carbon-hydrogen bond which is a stronger bond compared to alkyl bonds present in chains B and C. Protein 5wze (*Pseudomonas aeruginosa*) containing four chains, A, B, C and D. The pre-molecular docking revealed that chain 'A' contains single conventional hydrogen bond credited to amino acid residue GLU 312 and another pi-pi bond on residue TRP 372. Chain 'B' is the only chain on the 5wze protein void of conventional hydrogen bonds. However, two carbon-hydrogen bonds were identified on residues GLU384 and HIS 243 with an additional single pi-pi bond on residue HIS 350. The bonds in the 'C' chain are revealed as present on residues ARG 351 which is a conventional hydrogen bond while the bonds on GLU 384 and HIS 354 are carbon-hydrogen bonds. This chain also contains a pi-pi bond on HIS 350 residues. A single hydrogen bond was identified on chain 'D' at residue LEU 356, whereas other residues MET 184, VAL 412 and LYS 176 are weak alkyl bonds. Chain 'C' was selected for the molecular docking with the ligands under this study due to its number of residues which could form conventional hydrogen bonds with the ligands and carbon-hydrogen bonds. 1dih (*E. coli*) is one of the proteins that was subjected to the effect of the sample on microorganisms. The biovia studies of the protein chain receptor sites revealed the presence of six conventional hydrogen bonds located on GLY 12, MET 17, GLY 102, THR 104, ALA 126 and PHE 129. Other potential weak interaction bonds are located on PHE 79, THR 80 and GLY 84. One of the goals of this work is to identify the effect of Potassium oxide on microorganisms which are targeted when formulating antiseptics like hand sanitizer. To this effect, 7rn1 protein (SARS-CoV-2) was elucidated using biovia for the presence of binding sites which could form interaction with the test ligands. The result revealed that conventional hydrogen bonds on GLY143 and GLU 166 residues were identified whereas, two weak bonds on residues ASN 142 and MET 165 were reported.

FIG. 5:5iip protein

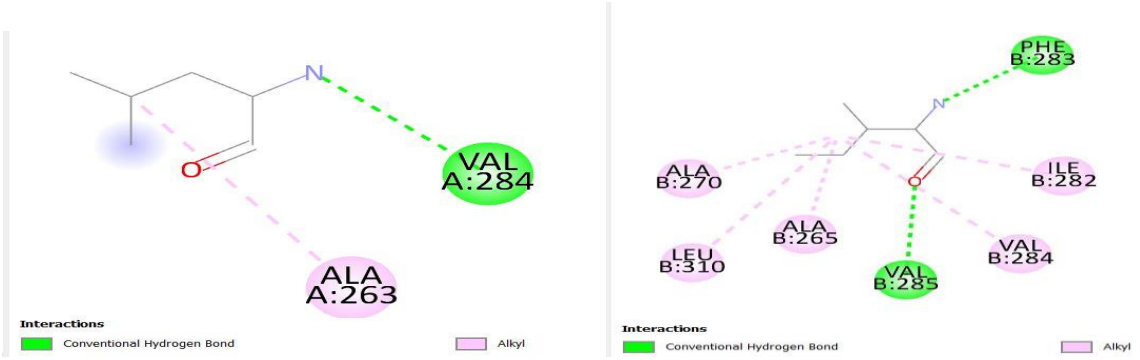

FIG. 6: Binding sites 5IIP chain A and B

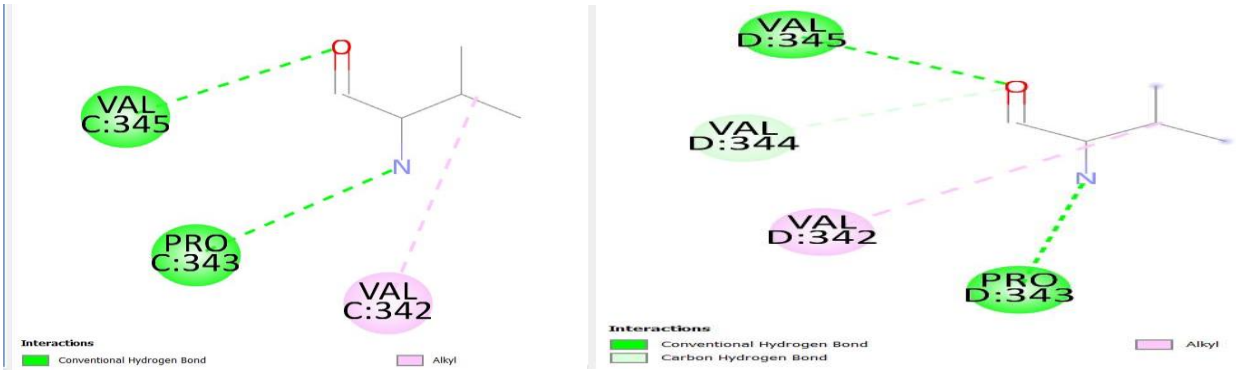

Fig. 7: Binding Site 5iip Chain C and D

Fig. 8 5wze protein

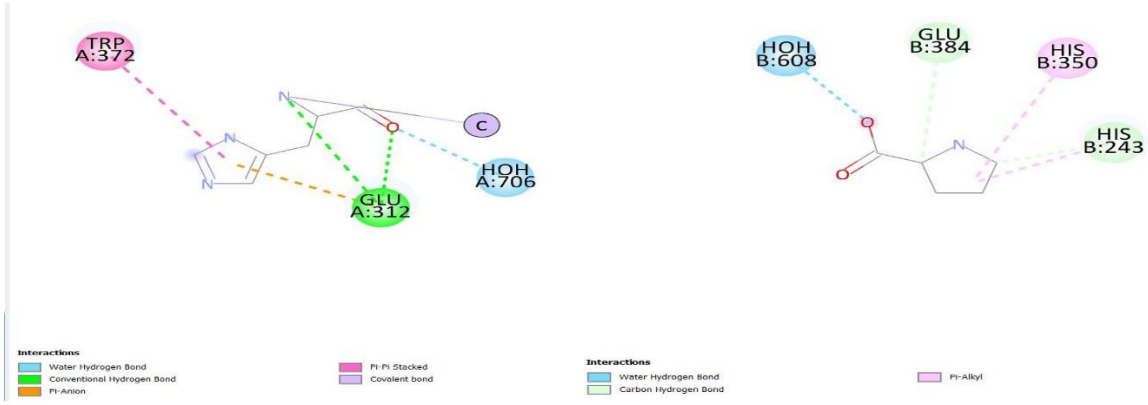

Fig. 9: Binding Sites 5wze Chain A and B

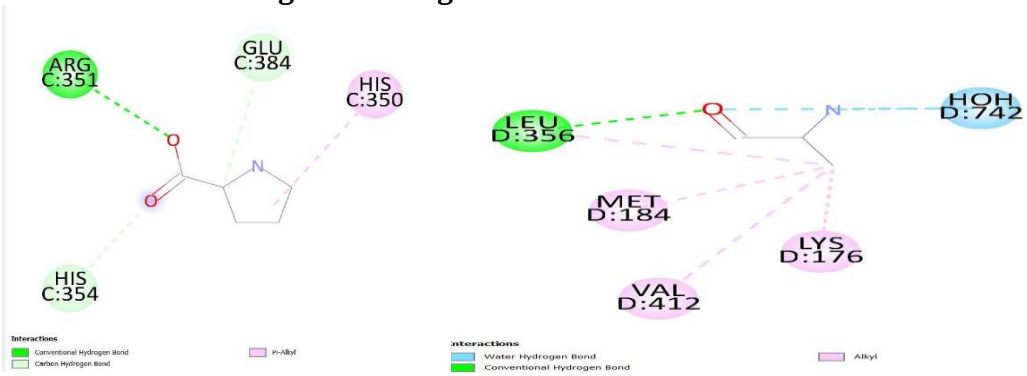

Fig. 10: Binding Sites 5wze Chain C and D

Fig. 11: 1dih protein

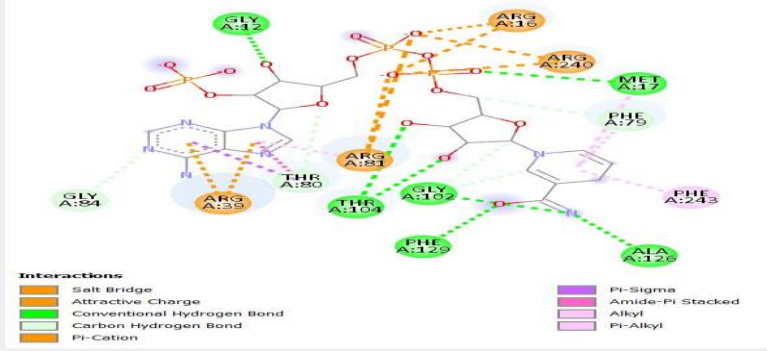

Fig. 12: Binding Sites 1dih

Fig. 13: 7rn1 protein

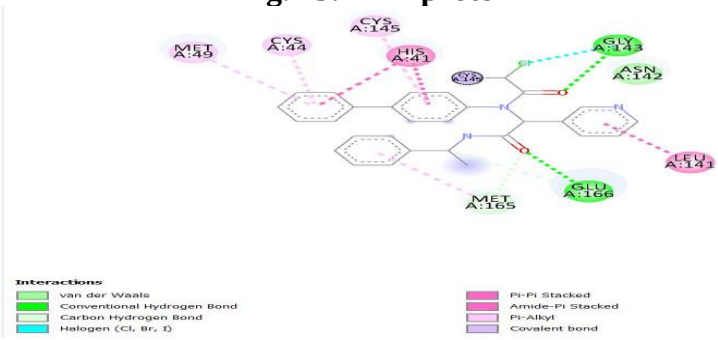

Fig. 13: Binding Sites 7rn1

3.5 Protein/Ligand interaction results

The result of the molecular docking between 5iip and three solvents containing Potassium Oxide (K_2O + Etol, K_2O + H_2O and K_2O + DMSO) revealed the presence of a single hydrogen bond involving the serine 330 unit of the receptor and the Oxygen atom of the sample K_2O (Fig. 14-16). This indicates that the solvent effect has an influence on the geometrical study of the compound and has no influence on the nature of the number of conventional hydrogen bonds formed. The protein 5wez shows the presence of four protein chains as shown in Fig. 6 and 7. However, only chain 'C' was selected for interaction with the sample in various solvents and the standard. The sample K_2O formed a single hydrogen bond with the protein 'C' at ASN 423 with the oxygen atom of the sample. Two electrostatic bonds were observed between potassium and GLU 431, and the second potassium atom and ASP 409. The interaction of the protein 5wze (Fig. 8) with the sample in the DMSO solution, revealed the presence of a single hydrogen bond between the oxygen atom of the K_2O and THR 382 residue (Fig. 7-19). Two carbon-hydrogen bonds were detected and revealed between the amino residue GLY 353, TRP 310 and the oxygen of the K_2O. this bond can only exist by sharing the lone pair of electrons located on the oxygen atom. The interaction at chain 'C' of 5wze protein is dominated by electrostatic interaction between the metal atom (Potassium) of the sample and ASP 166 and 49 amino residues, whereas, a single conventional hydrogen bond is formed between the oxygen atom of the sample compound and ASP 49 amino residue of the protein chain. 1dih protein (Fig. 10) has the most successful conventional

hydrogen bond of all the proteins of bacteria subjected to this test. The protein-ligand docking revealed the presence of these bonds between VAL 131, GLY 132 and SER 130 and the oxygen atom of the ligand (K_2O+H_2O) Fig. 20. Similar bonds were established when the sample was prepared in ethanolic and DMSO solutions as shown in Fig. 21-22. This shows that the interaction between the protein 1dih and potassium oxide is independent of these solvents.

Interaction between SARS-CoV-2 (7rni) (Fig. 12) and K_2O+Etol resulted in the formation of 4 hydrogen bonds, which indicates moderately high activity of the sample + Etol solution on SARS-CoV-2 virus 7rn1. Interestingly, some of these bonds are complexed around the same amino acid residue of the protein. This type of interaction is revealed between THR 111 which presented three conventional hydrogen bonds were one of the residues is the proton donor and the other two are the proton acceptor. Similar bonding was observed between the 7rni protein with K_2O+H_2O, except that, only 2 hydrogen bonds were observed when the DMSO sample solution was used. This work also revealed the effect of solvent type on the susceptibility of the 7 rn1 virus.

The standard in this work, Benzalkonium chloride has been compared with the sample under study for various microbial activities. The test microorganisms are proteins; 5iip, 5wze, 1dih and 7rni, these organisms show no conventional hydrogen bonds available as expressed by the molecular docking result (Fig. 26-29). However, a weak alkyl hydrogen bond was identified between GLU 315 and an alkyl group of the chain of this compound. Other weak interactions include; ALA 127, and PRO 227 identified in 5iip, 1dih and 5wze proteins respectively. The interaction between the standard (Benzalkonium chloride) and the SARS-CoV-2 protein 7rn1, also resulted in significant bonding as a result of the absence of conventional hydrogen bonding. However, two weak hydrogen alkyl bonds were identified.

From the above results presented, it can be deduced that, the sample (potassium oxide), which is a component of corn cob ash crystals does not have high activities on the tested microorganisms as revealed by both the experimental and molecular docking results. Therefore, this compound may not yield acute relief of symptoms of diseases caused by these microorganisms. Notwithstanding this result, the compound can be used as an antiseptic for cleansing surfaces where weak interactions would be sufficient to prevent bacteria and virus growth. In another development, the sample compound in all the solutions shows significant activities when docked against the SARS-CoV-2 protein 7rni. This finding indicates that the sample can be used in formulating hand sanitisers and other antiseptics which could possess no or little adverse effect.

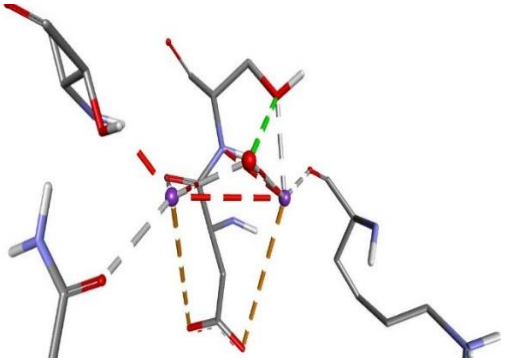

Fig. 14: K_2O+Etol+5iip, interaction

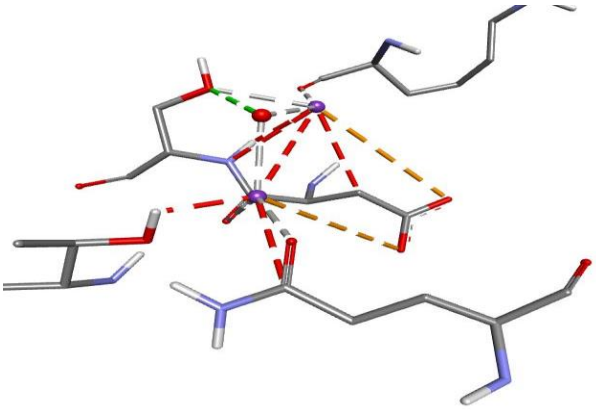

Fig. 15: K_2O+H_2O+5iip interaction

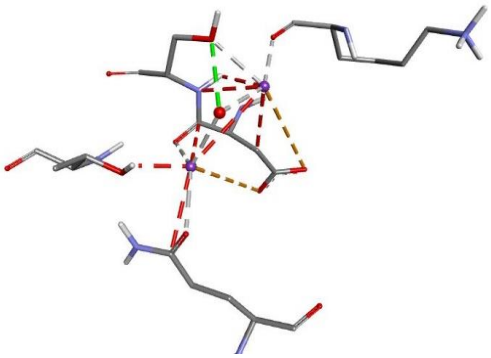

Fig. 16: K_2O+DMSO+5iip interaction

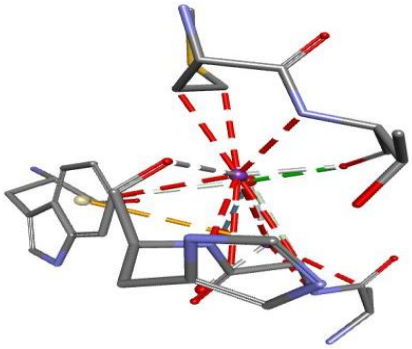

Fig. 17: K_2O+DMSO+5wze interaction

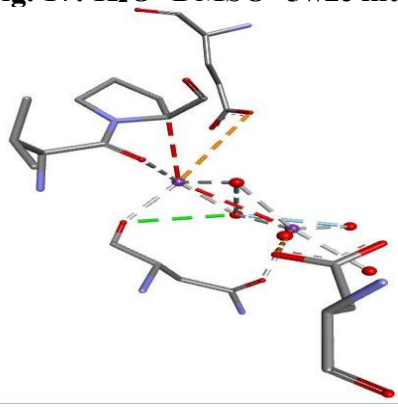

Fig. 18: K_2O+H_2O+5wze interaction

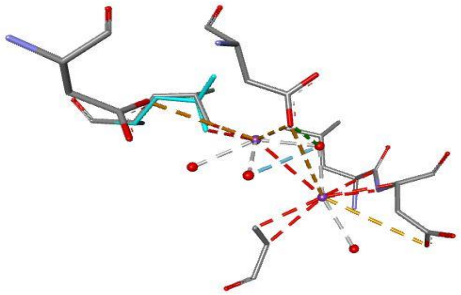

Fig. 19: K_2O+Etol+5wze interaction

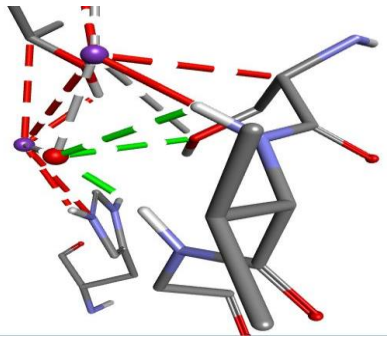

Fig. 20: K_2O+H_2O+1dih interaction

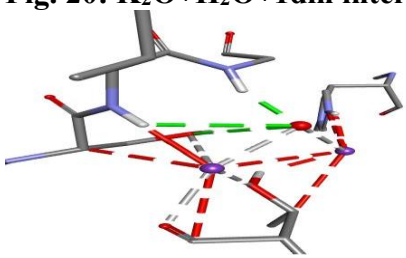

Fig. 21: K_2O+Etol+1dih interaction

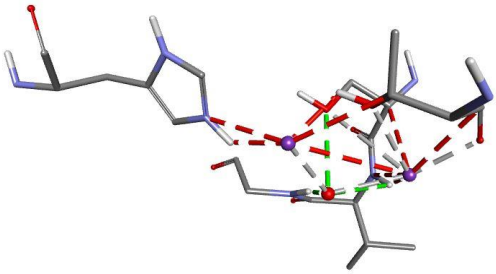

Fig. 22: K_2O+DMSO+1dih interaction

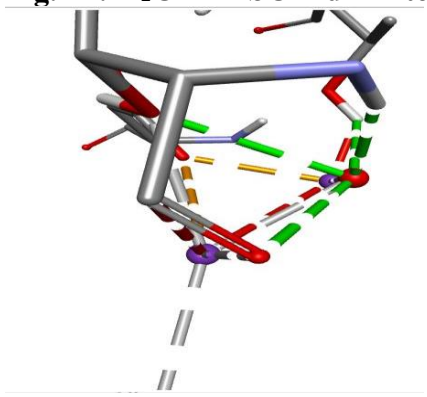

Fig. 23: K_2O+Etol+7mi interaction

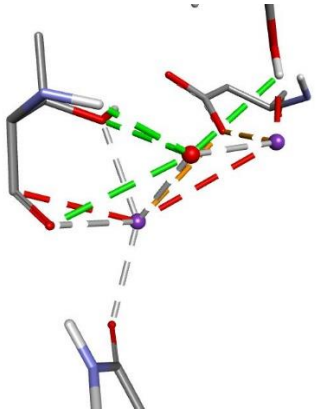

Fig. 24: K_2O+H_2O+7mi interaction

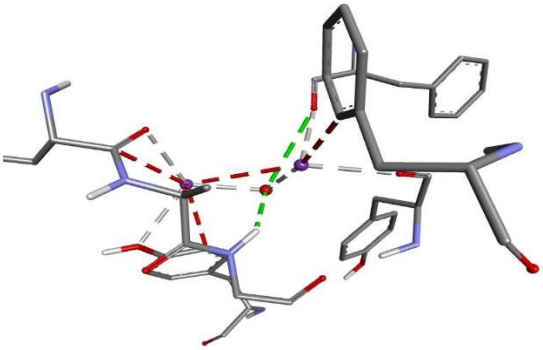

Fig. 25: K_2O+DMSO+7mi interaction

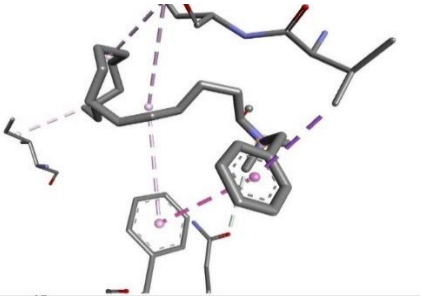

Fig. 26: Benzalkonium Chloride +5iip interaction

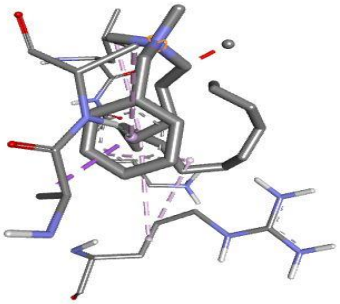

FIG. 27: Benzalkonium Chloride +1dih interaction

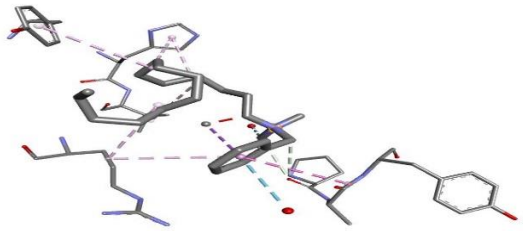

FIG. 28: BENZALKONIUM Cl +5wze interaction

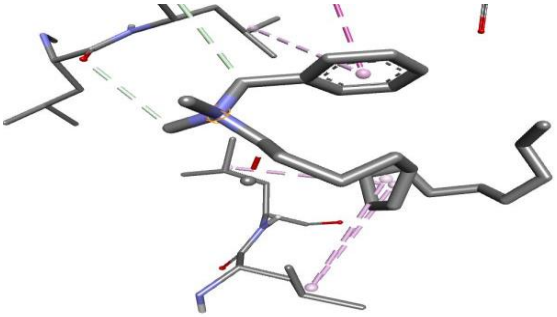

FIG. 29: BENZALKONIUM Cl +7mi interaction

4.0 Conclusion

This study looked closely at the antibacterial and disinfection properties of crystals of potassium oxide made from corncob ash. The results of the experimental investigation showed that potassium oxide (K_2O), together with other inorganic elements produced during burning and crystallization, makes up the majority of the crystals in corncob ash. Antimicrobial susceptibility testing revealed that Potassium oxide and Benzalkonium chloride had a little amount of action against *Staphylococcus aureus*, but that the usual medication, ampicillin, had a higher amount of activity against all of the examined bacteria.
Density Functional Theory (DFT) geometric analysis sheds light on the structure and reactivity of the chemical. The potassium oxide molecule's bond lengths and angles were dramatically affected by the presence of several solvents, demonstrating the value of taking the compound's behaviour in various environments into account.

The stability and limited reactivity of the chemical were discovered by analysis of its HOMO-LUMO orbitals and energy levels. The substance did, however, show notable interactions with the SARS-CoV-2 protein, suggesting the possibility of using it in the creation of antiseptics and hand ssanitisers to prevent viral transmission. This can also be a perfect substitute for alcohol-based hand sanitiser which has adverse side effects and in order religion considered abominable when used.

The compound's interactions with particular protein residues of the examined microorganisms were further supported by molecular docking investigations. Potassium oxide had a significant binding affinity for the SARS-CoV-2 protein, suggesting its possible use in antiseptic formulations that aim to stop viral transmission, even though its action against the chosen bacteria was not as strong as that of the conventional medicine.

Finally, due to its considerable interactions with microbes, potassium oxide made from crystals of corn cob ash may be used as an additional antiseptic agent for surface cleaning. Its antibacterial action, however, was not as strong as the antibiotic as a standard against the tested bacteria. However given the ongoing epidemic, the compound's interactions with the SARS-CoV-2 protein open up new avenues for its usage in creating antiseptics to thwart viral transmission.

The antibacterial characteristics of potassium oxide and its prospective use as an antiseptic agent are crucial insights provided by this work. To fully realize its promise in the area of hygiene and disease prevention, more study is required to examine its broader antibacterial efficacy and safety profiles. Additionally, examining its compatibility with various formulations and considering potential combination therapies could improve its efficiency and address the problems associated with antiseptic resistance. Potassium oxide from corn cob ash crystals shows promise as a viable option for next-generation antiseptic and disinfection formulations, which are needed in light of the rising concern over infectious diseases and the need for sustainable alternatives being sourced from agricultural waste.

5.0 Acknowledgement

The Authors wish to acknowledge the support provided by the National Open University of Nigeria, Senate Research Grant for sponsoring the cost of this entire research

5.0 References

Ahmad, M. S., Fatath, A. M., El-Nesr, A. K., & Ramadan, M. (2018). Nosocomial Antiseptics and Disinfectants Resistant Bacteria: microbiological and histopathological studies. *Journal of Veterinary Medical Research*, 25(2), 283–304.

Akita, S., Fujioka, M., Akita, T., Tanaka, J., & Masunaga, A. (2022). Effects of Hand Hygiene Using 4% Chlorhexidine Gluconate or Natural Soap During Hand Rubbing Followed by Alcohol-Based 1% Chlorhexidine Gluconate Sanitizer Lotion in the Operating Room. *Advance in Wound Care*, 11, 1, pp. 1–9.

Chen, B., Han, J., Dai, H., & Jia, P. (2021). Biocide-tolerance and antibiotic-resistance in community environments and risk of direct transfers to humans: Unintended consequences of community-wide surface disinfecting during COVID-19. *Environmental Pollution*, 283, 117074, https://doi.org/10.1016/j.envpol.2021.117074

Eddy, N. O. & Ita, B. I. (2011). Experimental and theoretical studies on the inhibition potentials of some derivatives of cyclopenta-1,3-diene. *International Journal of Quantum Chemistry* 111, 14, pp. 3456-3473. doi:10.1002/qua.

Eddy, N. O., Ukpe, R. A., Ameh, P., Ogbodo, R., Garg, R. & Garg, R. (2023). Theoretical

nd experimental studies on photocatalytic removal of methylene blue (MetB) from aqueous solution using oyster shell synthesized CaO nanoparticles (CaONP-O). *Environmental Science and Pollution Research*, https://doi.org/10.1007/s11356-022-22747-w

Elegbede, J. A., Ajayi, V. A. & Lateef, A. (2021). Microbial valorization of corncob: Novel route for biotechnological products for sustainable bioeconomy. *Environmental Technology and Innovation*, 24, 102073. https://doi.org/10.1016/j.eti.2021.102073

Eno, E., Shagal, H. M., Godfrey, C. O., Ekong, E. J., Gber, E. T., Benjamin, I., & Louis, H. (2023). Computational study of the interaction of metal ions (Na+, K+, Mg2+, Ca2+, and Al3+) with Quercetin and its antioxidant properties. *Journal of the Indian Chemical Society*, 100, 3, doi: 10.106/j.jics.2023.101059.

Ghafoor, D., Khan, Z., Khan, A., Ualiyeva, D., & Zaman, N. (2021). Excessive use of disinfectants against COVID-19 poses a potential threat to living beings. *Current Research in Toxicology*, 2, pp. 159-168.

Hernandes, E. S., Mello, C. A., Sant'Ana, J. J., Soares, S. V., Cassiolato, V., GarciaB, L., & Cardoso, L. C. (2004). The Effectiveness of Alcohol Gel and Other Hand-Cleansing Agents Against Important Nosocomial Pathogens. *Brazilian Journal of Microbiology*, 35, pp. 33-39.

Kareem, S. O., Akpan, I., & Alebiowu, O. O. (2010). Production of citric acid by Aspergillus niger using pineapple waste. *Malaysian Journal of Microbiology*, 6, 2, pp. 161-165.

Kistan, A., Kanchana, V., Parthiban, E., Vadivel, S., & Sridhar, B. (2023). Study on flexural behaviour of polypropylene fibre reinforced fly ash concrete beam. *Materials Today: Proceedings*.

Laohalidonand, K., Kongkaew, N., & Kerdsuwan, S. (2017). Assessing the feasibility of using the heat demand-outdo Gasification Behavior Study of Torrefied Empty Corn Cobs. *Energy Procedia*, 138, 175–180.

Ma, C., Xia, Z., Sacco, M. D., Hu, Y., Townsend, J. A., Meng, X., ... & Wang, J. (2021). Crystal structure of the SARS-CoV-2 (COVID-19) main protease in complex with inhibitor Jun9-62-2R. *Journal of the American Chemical Society*, 143, pp. 20697-20709.

McDonnell, G. & Rusell, D. A. (1999). Antiseptics and Disinfectants: Activity, Action, and Resistance. *Clinical Microbiology Reviews*. 12, 1, pp. 147-179.

Melo-Silveira, R. F., Fidelis, G. P., Costa, M. S. S. P., Telles, C. B. S., Dantas-Santos, N., Elias, S. O., ... & Rocha, H. A. O. (2011). In Vitro Antioxidant, Anticoagulant and Antimicrobial Activity and in Inhibition of Cancer Cell Proliferation by Xylan Extracted from Corn Cobs. *International Journal of Molecular Science*, 13, 1, pp. 409–426.

OBI, F. C. (1990). Use of X-Ray Fluorescence Spectrometry to Determine Trace Elements in Graphite. *Nigerian Journal of Technology*, 14, 1, pp. 1-4.

Olafusi, S. O., Kupolati, K. W., Sadiku, R. E., Snyman, J., & Ndambuki, M. J. (2018). Characterization of Corncob Ash (CCA) As a Pozzolanic Material. *International Journal of Civil Engineering and Technology*, 9, 12, pp. 1016-1024.

Peng, C. T., Liu, L., Li, C. C., He, L. H., Li, T., Shen, Y. L., ... & Bao, R. (2017). Structure-Function Relationship of Aminopeptidase P from Pseudomonas aeruginosa. *Frontiers in Microbiology*, 8, pp. 2385-2385.

Schulte, L. E., Schuster, C. F., Tosi, T., Campeotto, I., Corrigan, R. M., Freemont, P. S., & Grundling, A. (2016). The second messenger c-di-AMP inhibits the osmolyte uptake system OpuC in Staphylococcus

aureus. *Science Signaling*, 9, 441, pp. https://doi.org/10.1126/scisignal.aaf7279.

Wojcieszak, D., Przybył, J., Czajkowski, Ł., Majka, J., & Pawłowski, A. (2022). Effects of Harvest Maturity on the Chemical and Energetic Properties of Corn Stover Biomass Combustion. *Materials (Basel)*, 15, 8, 2831. doi:10.3390/ma15082831.\

Yao, X., Zu, K., Yan, F., & Liang, Y. (2017). The Influence of Ashing Temperature on Ash Fouling and Slagging Characteristics during Combustion of Biomass Fuels. *BioResources*, 12, 1, pp. 1593-1606.

Compliance with Ethical Standards
Declarations

The authors declare that they have no conflict of interest.

Data availability

All data used in this study will be readily available to the public.

Consent for publication
Not Applicable

Availability of data and materials

The publisher has the right to make the data public.

Competing interests

The authors declared no conflict of interest.

Funding
This work was funded by the Senate Research Grant of the National Open University of Nigeria as awarded and supervised by the Directorate of Research Administration of the University.

Authors' Contributions

Dr. Henrietta Ijeoma Kelle, is the lead researcher who designed the work and sourced for the funds utilized for this work. This author also put the literature review together and was involved in the analysis of the samples
Dr. Musa Runde, is the corresponding author who analyzed the data and wrote the discussions in this work